A New Method to Investigate the Progressive Damage of Imperfect Composite Plates Under In-Plane Compressive Load

S. A. M. Ghannadpour*, M. Shakeri

New Technologies and Engineering Department, Shahid Beheshti University, G.C, Tehran, Iran

ABSTRACT: Numerous studies have been conducted for failure criteria of fiber reinforced composites. The aim of this study is to present a new computational and mathematical method to analyze the progressive damage and failure behavior of composite plates containing initial geometric imperfections under uniaxial in-plane compression load. A new methodology is presented based on collocation method in which the interested domain is discretized with Legendre-Gauss-Lobatto nodes. In order to avoid an excessive number of nodes, an appropriate weight coefficient is considered for each node. The method is based on the first order shear deformation theory and small displacement theory. Several failure criteria, including Maximum stress, Hashin and Tsai-Hill, are used to predict the failure mechanisms. The stiffness degradation is carried out by instantaneous and complete ply degradation model. Two different types of boundary conditions are considered in this study. The effects of thickness, initial imperfections, and boundary conditions are studied, as well. The results are compared with the previously published data. It is found that the boundary conditions have significant effects on the ultimate strength of imperfect composite plates.

1- Introduction

Thin-walled structures have regularly been used in structural design. Composite plates are one of the thin-walled structures that can be optimized to carry in-plane compressive loads beyond their buckling load. Several laminate theories have been exploited to explain composite laminated plates' behavior. The Classical Laminated Plate Theory (CLPT) is an extension of classical plate theory based on the Kirchhoff hypothesis for isotropic plates [1, 2]. An improvement on the CLPT leads to the creation of the First-order Shear Deformation Theory (FSDT) which accounts for the transverse shear effects in relatively thick laminates[3, 4].

For moderately thick composite plates with geometric imperfection, linear, nonlinear and post-buckling analyses without taking the account of damage and also material degradations are very conservative analyses that give uncertain estimates of critical loads. Hence, damage analyses and ultimate strength of such structures have been of considerable research interest. In the field of buckling and post-buckling analyses, many researchers have extensively investigated these behaviors for composite beams and plates without considering the damage effects. Turvey and Marshall [5] and Argyris and Tenek [6] published excellent reviews on past research of buckling and post-buckling of structures using different methods.

Finite Strip Method (FSM) is an applicable method for buckling and post-buckling analyses of plates and plates structures. Finite strip method is based on the discretization of the domain into longitudinal strips which interpolates the behavior in the longitudinal direction by different functions, depending on different versions of FSM and in the transverse direction by polynomial functions. Cheung [7] may be considered as the pioneer who first proposed the concept of FSM. Cheung established FSM for the analysis of simply supported plates. The study presented by Smith and Sridharan [8] proposed FSM for the buckling of the isotropic plate under the edge loading. Recently, Ovesy, Ghannadpour, and their co-workers have made several contributions by developing two variants of finite strip methods, namely the full-energy and semi-energy finite strip approaches. Two different versions of finite strip method, namely spline and semi-analytical methods are also developed by them for predicting the response of rectangular laminates with a symmetric and non-symmetric form of initial imperfection [9]. They used both formulations for predicting the geometrically non-linear response of channel sections with simply supported ends when subjected to uniform end-shortening in their plane [10]. To extend their works, they developed a high accuracy finite strip for the buckling and post-buckling analyses of moderately thick symmetric cross-ply composite plates based on FSDT [11].

Furthermore, many other methods were employed to investigate composite plates behavior subjected to compressive loads such as a new class of numerical methods called meshless methods [12]. These methods have attracted the attention of many researchers in recent years due to the fact that meshless methods do not require a mesh to discretize the problem domain as in the finite element method and require only a scattered set of nodes to model the domain of interest Liew et al. [13, 14] studied buckling and post-buckling of laminates using the moving least-squares differential quadrature and mesh-free kp-Ritz method. Also, Liew et al. [15] published a review of meshless methods and their applications in the buckling analysis of laminated

Corresponding author, E-mail: a_ghannadpour@sbu.ac.ir

and functionally graded plates. More recently, Ghannadpour and Barekati [16] investigated the post-buckling behavior of composite plates using Chebyshev techniques by considering initial imperfection effects.

As noted before, all the above research works, have investigated the linear and nonlinear behaviors of plates without considering the effects of damage or failure and therefore the obtained results are very conservative. On the other hand, as was observed, all the mentioned studies have been carried out by different numerical or semi-analytical methods. However, strength analyses of metal plates and damage analyses of composite plates are usually carried out using FEM in which the storage required is extremely large, and the computational time is too lengthy [17]. Only a limited number of such analyses have been implemented by other numerical or semi-analytical methods.

Several simplified semi-analytical methods have been purposed by Brubak et al. [18-21] to investigate the strength of stiffened and unstiffened metal plates with imperfection and cutout. .Accelerated analysis techniques were proposed by Orifici et al. [22] using FEM tools such as ABAQUS to model the degradation and fracture mechanics of composite stiffened fuselage panel in a post-buckling regime. Some experimental works compared to FEM analysis can be found on the ultimate strength of composite plates such as study investigated by Hayman et al. [23]. These studies have included a parametric study of ultimate strength analysis of rectangular simply supported composite plates with different geometrical imperfections. Yang et al. [24-26] have recently carried out valuable studies using the simplified method to predict an ultimate strength of composite plates with different initial imperfection values under in-plane compressive loads.

In the present paper, a simplified progressive damage model is developed to predict the ultimate strength of imperfect composite plates with different boundary conditions under in-plane compressive load based on the Ritz method. The advantage of Ritz method is that the unknown displacements do not require to satisfy all the specified boundary conditions. In this method, the approximating functions are sufficient to meet only geometric boundary conditions and the natural boundary conditions are met automatically. A new methodology is presented based on the collocation method in which the interested domain is discretized with Legendre-Gauss-Lobatto nodes. The method is based on the first order shear deformation theory and small displacement theory. Several failure criteria, including Maximum stress, Hashin and Tsai-Hill, are used to predict the failure mechanisms. The stiffness degradation is carried out by instantaneous and complete ply degradation model. Two different types of boundary conditions are considered in this study. The effects of thickness, initial imperfections, and boundary conditions are studied. The accuracy of the present work is examined by comparing the numerical results with the previous studies.

2- Theoretical formulations

A typical rectangular laminated plate of dimensions of $a \times b$ and total thickness h with an initial geometric imperfection w_i in the center of plate and in the z-direction is shown in Fig. 1 where Ω is the domain occupied by the plate mid-plane. The laminate is subjected to in-plane compressive load on the edge $x = a/2$ in the x-direction called N_x. Two different types of boundary conditions are considered that will be mentioned

later. The laminates are assumed to be moderately thick, thus theoretical formulations are based on the first order shear deformation theory (FSDT).
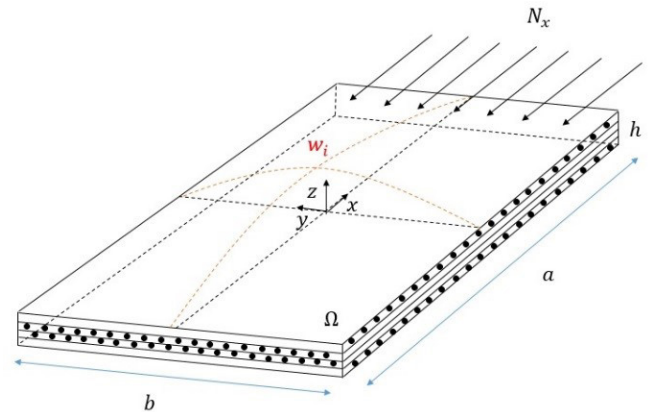

Fig. 1. A typical imperfect rectangular laminated plate

The total potential energy Π consists of the strain energy of the plate U and potential energy of external forces V. Therefore, the total potential energy can be obtained by:

$$\Pi = \mathcal{U} + \mathcal{V} \tag{1a}$$

$$\mathcal{U} = \frac{1}{2} \iiint_V \boldsymbol{\sigma}^T e \, dV$$
$$= \frac{1}{2} \iint_\Omega \int_z \boldsymbol{\sigma}^T e \, dz \, d\Omega \tag{1b}$$
$$= \frac{1}{2} \iint_\Omega \boldsymbol{\varepsilon}^T \boldsymbol{S} \boldsymbol{\varepsilon} \, d\Omega$$

$$= -\iint_\Omega \left(\boldsymbol{\varepsilon}_p^T - \boldsymbol{\varepsilon}_{nl}^T - \bar{\boldsymbol{\varepsilon}}_p^T \right) \tilde{\mathcal{F}} \, d\Omega \tag{1c}$$

Where $\tilde{F}$ is the external force vector on the plate $\tilde{F} = \langle N_x \, N_y \, N_{xy} \rangle^T$. Also $\boldsymbol{\varepsilon}_p$, $\boldsymbol{\varepsilon}_{nl}$ and $\bar{\boldsymbol{\varepsilon}}_p$ are linear, nonlinear and imperfection strains vectors, respectively. In Eq. (1) a stiffness matrices $\boldsymbol{S}$ is defined as:

$$\boldsymbol{S} = \begin{bmatrix} \boldsymbol{A}_p & \boldsymbol{B} & 0 \\ \boldsymbol{B} & \boldsymbol{D} & 0 \\ 0 & 0 & \boldsymbol{A}_n \end{bmatrix} \tag{2}$$

In which $\boldsymbol{A}_p$, $\boldsymbol{B}$, $\boldsymbol{D}$ and $\boldsymbol{A}_n$ are the generalized stiffness matrices, which are extensional stiffness matrix, extensional-bending stiffness matrix, bending stiffness and interlaminar shear stiffness matrices, respectively. They can be computed by the following equations.

$$\left(\boldsymbol{A}_p, \boldsymbol{B}, \boldsymbol{D} \right) = \sum_{k=1}^{N_\ell} \int_{h_{k-1}}^{h_k} \bar{\boldsymbol{Q}}_p^{(k)} \left(1, z, z^2 \right) dz \tag{3a}$$

$$\boldsymbol{A}_n = K \sum_{k=1}^{N_\ell} \int_{h_{k-1}}^{h_k} \bar{\boldsymbol{Q}}_n^{(k)} dz \tag{3b}$$

To describe the deformation of a laminated plate, displacement

vector $d=\langle d_x\ d_y\ d_z\rangle^T$ is considered and expressed by

$$d = u + z\vartheta + \overline{u} \tag{4}$$

Whose components of displacement vector are given by:

$$d_x(x,y,z) = u(x,y) + z\,\varphi_x \tag{5a}$$

$$d_y(x,y,z) = v(x,y) + z\,\varphi_y \tag{5b}$$

$$d_z(x,y,z) = w(x,y) + \overline{w}(x,y) \tag{5c}$$

Where $u=\langle u\ v\ w\rangle^T$, $\vartheta=\langle \varphi_x\ \varphi_y\ 0\rangle^T$ and $u=\langle 0\ 0\ \overline{w}\rangle^T$. According to the FSDT [27], (u,v,w) are in-plane displacement of mid-plane, and φ_x and φ_y denote the rotations of a transverse normal about axes parallel to the y and x axes, respectively and $\overline{w}$ is initial geometric imperfection of the laminate in the form of a single half sine-wave in both directions.

The vector of Green's strains e in a total Lagrangian formulation is written as

$$e = \langle e_{xx}\ \ e_{yy}\ \ e_{xy}\ \ e_{xz}\ \ e_{yz}\ \ e_{zz}\rangle^T$$
$$= \begin{Bmatrix} e_p \\ e_n \end{Bmatrix} \tag{6}$$

Where e_p and e_n are in-plane and out-of-plane component vectors with subscripts p and n, respectively. By inserting geometric nonlinearity into the von Karman sense, the strain-displacement relations are given as:

$$e_p = \varepsilon_p + \varepsilon_{nl} + \overline{\varepsilon}_p + z\kappa$$
$$= \mathcal{D}_p u + \frac{1}{2}\left(\mathcal{D}_p \otimes w\right)\mathcal{D}_n u + \left(\mathcal{D}_p \otimes \overline{w}\right)\mathcal{D}_n u + z\,\mathcal{D}_p\vartheta \tag{7a}$$

$$e_n = \gamma = \mathcal{D}_n u + \vartheta \tag{7b}$$

Where $\otimes$ denotes the Kronecker product. Also, Eq. (7) defines the plate strain vectors that are the in-plane strains vector ε_0, the curvatures vector κ and the shear strains vector γ. The structural model in this study is based on the assumption of small deflection theory, therefore the nonlinear and imperfection strains vectors $(\varepsilon_{nl}, \overline{\varepsilon}_p)$ are neglected henceforth. Differential operators $\mathcal{D}_p$ and $\mathcal{D}_n$ can be defined as

$$\mathcal{D}_p = \begin{bmatrix} \dfrac{\partial}{\partial x} & 0 & 0 \\[2mm] 0 & \dfrac{\partial}{\partial y} & 0 \\[2mm] \dfrac{\partial}{\partial y} & \dfrac{\partial}{\partial x} & 0 \end{bmatrix} \tag{8a}$$

$$\mathcal{D}_n = \begin{bmatrix} 0 & 0 & \dfrac{\partial}{\partial x} \\[2mm] 0 & 0 & \dfrac{\partial}{\partial y} \\[2mm] 0 & 0 & 0 \end{bmatrix} \tag{8b}$$

The mechanical state is described by the stress vector σ, which can be written as

$$\sigma = \langle \sigma_{xx}\ \ \sigma_{yy}\ \ \sigma_{xy}\ \ \sigma_{xz}\ \ \sigma_{yz}\ \ \sigma_{zz}\rangle^T = \begin{Bmatrix} \sigma_p \\ \sigma_n \end{Bmatrix} \tag{9}$$

3- Displacement Fields and Boundary Conditions

The laminates under consideration have two different types of boundary conditions as represented in Fig. 2 and Fig. 3. As shown in this figures, for both types of boundary conditions, the in-plane displacement in x-direction at $x=-a/2$ and in y-direction at $y=-b/2$ are completely restricted and in the opposite edges uniform movements are allowed and then all four edges of the plates are being held straight.
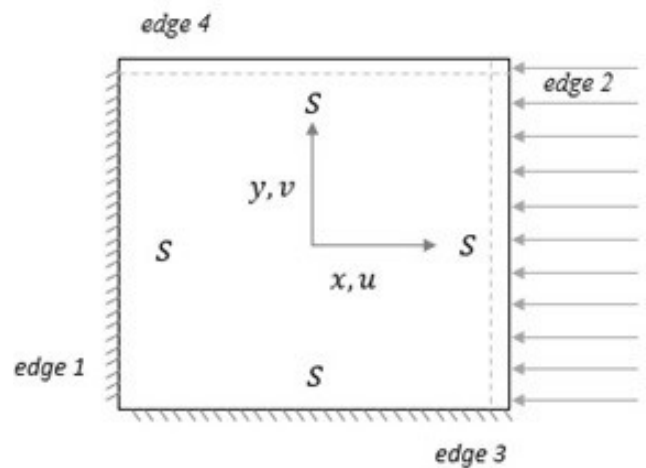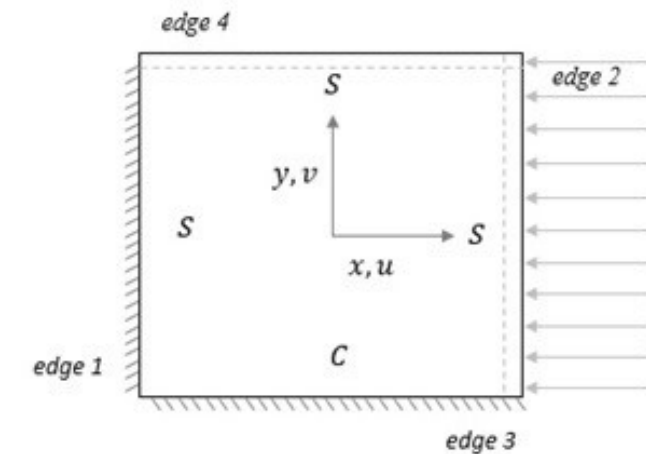

Fig. 2. Boundary conditions Type A

Fig. 3. Boundary conditions Type B

However, as can be seen, the labeling schemes are included in these figures to assign the related boundary conditions. The letter S refers to simply supported boundary condition and the letter C refers to clamped boundary condition on the specified edge. Therefore, the two aforementioned boundary conditions are different from the viewpoint of out-of-plane boundary conditions. The details of edges conditions for both Type A and Type B are expressed in Table 1.

Since the Rayleigh-Ritz technique is used in this study, the approximated displacement fields have to satisfy only

Table 1. Details of edges conditions for both Type A and Type B

Displacement fields	Edge boundary condition			
	edge 1	edge 2	edge 3	edge 4
u	Held	Straight	Free	Free
v	Free	Free	Held	Straight
w	Held	Held	Held	Held
φ_x	Free	Free	Held	Held
φ_y	Held	Held	Free* Held**	Free

* For boundary condition type A
** For boundary condition type B

the aforementioned essential boundary conditions. The approximation of displacement fields is performed by Legendre basis functions P. Legendre polynomials are one of the most powerful mathematical series for numerical methods. Legendre basis functions or Legendre polynomials are solutions to the following Legendre differential equation:

$$\frac{d}{dx}\left[\left(1-x^2\right)\frac{d}{dx}P_n\left(x\right)\right]+n\left(n+1\right)P_n\left(x\right)=0 \qquad (10)$$

Also, Legendre polynomials satisfy the three-term recursion as:

$$P_{n+1}\left(x\right)=\frac{2n+1}{n+1}xP_n\left(x\right)-\frac{n}{n+1}P_{n-1}\left(x\right) \qquad (11)$$

Where $P_0(x)=1$ and $P_1(x)=x$. Therefore, the displacement fields of the problem can be approximated by the following relations.

$$u_0 = f_u\left(\bar{x}\right)g_u\left(\bar{y}\right)\sum_{i=1}^{N_t}\sum_{j=1}^{N_t}u_{ij}P_{i-1}\left(\bar{x}\right)P_{j-1}\left(\bar{y}\right)$$
$$+F_u\left(\bar{x}\right)G_u\left(\bar{y}\right)u_c \qquad (12a)$$

$$v_0 = f_v\left(\bar{x}\right)g_v\left(\bar{y}\right)\sum_{i=1}^{N_t}\sum_{j=1}^{N_t}v_{ij}P_{i-1}\left(\bar{x}\right)P_{j-1}\left(\bar{y}\right)$$
$$+F_v\left(\bar{x}\right)G_v\left(\bar{y}\right)v_c \qquad (12b)$$

$$w = f_w\left(\bar{x}\right)g_w\left(\bar{y}\right)\sum_{i=1}^{N_t}\sum_{j=1}^{N_t}w_{ij}P_{i-1}\left(\bar{x}\right)P_{j-1}\left(\bar{y}\right) \qquad (12c)$$

$$\varphi_x = f_{\varphi_x}\left(\bar{x}\right)g_{\varphi_x}\left(\bar{y}\right)\sum_{i=1}^{N_t}\sum_{j=1}^{N_t}\varphi_{x\,ij}P_{i-1}\left(\bar{x}\right)P_{j-1}\left(\bar{y}\right) \qquad (12d)$$

$$\varphi_y = f_{\varphi_y}\left(\bar{x}\right)g_{\varphi_y}\left(\bar{y}\right)\sum_{i=1}^{N_t}\sum_{j=1}^{N_t}\varphi_{y\,ij}P_{i-1}\left(\bar{x}\right)P_{j-1}\left(\bar{y}\right) \qquad (12e)$$

where $\bar{x}$ and $\bar{y}$ are non-dimensional coordinates defined as $2x/a$ and $2y/b$, respectively. Boundary functions are chosen to ensure the fulfillment of the essential boundary conditions mentioned in Table 1. It can be defined as in Table 2.

Table 2. Functions of boundary conditions

Boundary function	Type A	Type B
$f_u(\bar{x})$	$(1-\bar{x}^2)/4$	$(1-\bar{x}^2)/4$
$g_u(\bar{y})$	$(1-\bar{y}^2)/4$	$(1-\bar{y}^2)/4$
$F_u(\bar{x})$	$(1+\bar{x})/2$	$(1+\bar{x})/2$
$G_u(\bar{y})$	1	1
$f_v(\bar{x})$	$(1-\bar{x}^2)/4$	$(1-\bar{x}^2)/4$
$g_v(\bar{y})$	$(1-\bar{y}^2)/4$	$(1-\bar{y}^2)/4$
$F_v(\bar{x})$	1	1
$G_v(\bar{y})$	$(1+\bar{y})/2$	$(1+\bar{y})/2$
$f_w(\bar{x})$	$(1-\bar{x}^2)/4$	$(1-\bar{x}^2)/4$
$g_w(\bar{y})$	$(1-\bar{y}^2)/4$	$(1-\bar{y}^2)/4$
$f_{\varphi_x}(\bar{x})$	1	1
$g_{\varphi_x}(\bar{y})$	$(1-\bar{y}^2)/4$	$(1-\bar{y}^2)/4$
$f_{\varphi_y}(\bar{x})$	$(1-\bar{x}^2)/4$	$(1-\bar{x}^2)/4$
$g_{\varphi_y}(\bar{y})$	1	$(1+\bar{y})/2$

4- Solution Procedure

In the current approach, the domain of plate is discretized by a set of nodes; therefore, the continuous integrals of total potential energy should be replaced by summations where they can be calculated over all nodes. For this purpose, Legendre-Gauss-Lobatto nodes are established here and can be obtained by solving the following equations:

$$\begin{cases} \bar{x}_\zeta \;:\; P'_{n-1}\left(\bar{x}_\zeta\right)=0 \\ \bar{y}_\eta \;:\; P'_{m-1}\left(\bar{y}_\eta\right)=0 \end{cases} \qquad (13)$$

The parameters n and m denote the number of nodes in x and y directions, respectively and $\bar{x}_\zeta$ and $\bar{y}_\eta$ are non-dimensional coordinates of ζth and η^{th} node in the x and y directions. Fig. 4 represents a scattered set of Legendre-Gauss-Lobatto nodes ($m \times n = 13 \times 13$) in a typical domain Ω.
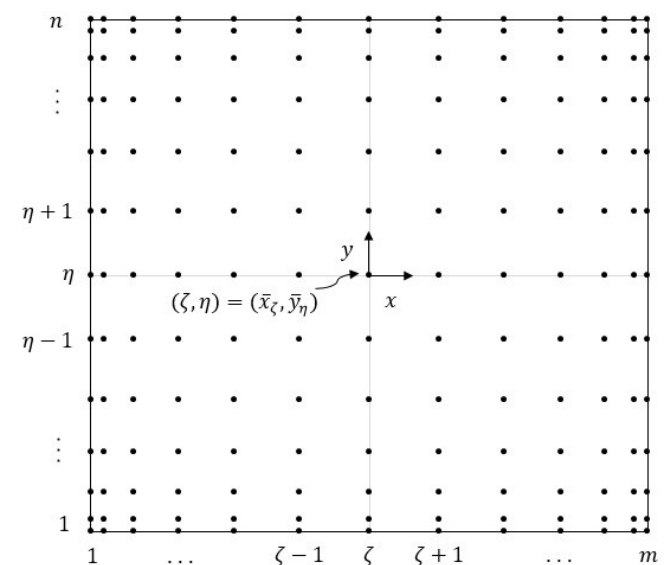

Fig. 4. Discretized plate model

In order to avoid an excessive number of nodes, an appropriate weight coefficient is considered for each node.

Therefore, the continuous integral of total potential energy after eliminating the constant factors is then converted to the following relation:

$$\Pi = \frac{1}{2} \int_{\Omega} \Pi^* (x, y) \, d\Omega$$

$$\Pi \approx \frac{1}{2} \sum_{i=1}^{N_P} \varpi_\zeta \omega_\eta \Pi^* (\bar{x}_i, \bar{y}_i) \tag{14}$$

Where $\langle \zeta, \eta \rangle$ indicates the ζth node in x direction and η^{th} node in y direction as represented in Fig. 4. The coefficients ϖ_ζ and ω_η are weight coefficients of nodes in x and y directions, respectively and they can be computed by:

$$\varpi_1 = \varpi_m = \frac{2}{m(m-1)};$$

$$\varpi_\zeta = \frac{2}{m(m-1)\left[P_{m-1}(\bar{x}_\zeta)\right]^2} \tag{15a}$$

$$\omega_1 = \omega_n = \frac{2}{n(n-1)};$$

$$\omega_\eta = \frac{2}{n(n-1)\left[P_{n-1}(\bar{y}_\eta)\right]^2} \tag{15b}$$

The unknown coefficients in displacement fields can be found by solving of equilibrium equations of the problem. Based on the principle of minimum potential energy, the equilibrium equations are obtained as below.

$$\frac{\partial \Pi}{\partial u_c} = \frac{\partial \Pi}{\partial v_c} = \frac{\partial \Pi}{\partial u_{ij}} = \frac{\partial \Pi}{\partial v_{ij}} = \frac{\partial \Pi}{\partial w_{ij}} = \frac{\partial \Pi}{\partial \varphi_{x_{ij}}} = \frac{\partial \Pi}{\partial \varphi_{x_{ij}}} = 0 \tag{16}$$

5- Progressive damage methodology

The methodology of progressive damage analysis, including the failure criteria and material degradation model, is described here.

In order to determine the failure load and the corresponding failure mode, a proper failure criterion should be established. Several failure criteria, including Maximum stress, Hashin and Tsai-Hill, are used to predict the failure mechanisms in this section.

In the maximum stress, criterion failure occurs when at least one of the stresses in fiber or matrix direction exceeds the corresponding strength value. This criterion can be presented as:

Fiber failure in tension ($\sigma_1 \geq 0$):

$$\sigma_1 > X_T \tag{17a}$$

Fiber failure in compression ($\sigma_1 < 0$):

$$|\sigma_1| > X_c \tag{17b}$$

Matrix failure in tension ($\sigma_2 \geq 0$):

$$\sigma_2 > Y_T \tag{17c}$$

Matrix failure in compression ($\sigma_2 < 0$):

$$|\sigma_2| > Y_c \tag{17d}$$

Here X_T and X_C denote tensile and compressive strengths of fiber and Y_T and Y_C are tensile and compressive strengths of matrix, the respectively. Failure happens when any of these modes reaches unity.

This failure criterion cannot consider the interaction among stress components. For this purpose, quadratic interaction criteria such as Tsai-Hill failure criterion have been developed. This criterion is similar to von Mises criterion for the plasticity of metals but adapted for orthotropic materials. Failure criteria are nothing more than curve fits for experimental data. Therefore, the following equation is proposed by Tsai-Hill for plane stress condition [28].

$$\left(\frac{\sigma_1}{X}\right)^2 - \frac{\sigma_1 \sigma_2}{X^2} + \left(\frac{\sigma_2}{Y}\right)^2 + \left(\frac{\tau_{12}}{S_{12}}\right)^2 - 1 = 0 \tag{18}$$

A disadvantage of Tsai-Hill criterion is that the mode of failure is not identified and Tsai-Hill criterion does not take into account the different behaviors in tension and compression, which is very important for polymer matrix composites. The strength values that are used in Tsai-Hill criterion have to be chosen for either the tensile or compressive strength value corresponding to the state of the stress of the problem.

The last failure criterion adopted in this study is Hashin failure criterion. This criterion includes four different damage functions which correspond to the different modes of failure namely fiber tension, fiber compression, matrix tension, and matrix compression. These criteria can be presented as:

Fiber failure in tension ($\sigma_1 \geq 0$):

$$F_f^T = \left(\frac{\sigma_1}{X_T}\right)^2 \tag{19a}$$

Fiber failure in compression ($\sigma_1 < 0$):

$$F_f^C = \left(\frac{\sigma_1}{X_C}\right)^2 \tag{19b}$$

Matrix failure in tension ($\sigma_2 \geq 0$):

$$F_m^T = \left(\frac{\sigma_2}{Y_T}\right)^2 + \left(\frac{\tau_{12}}{S_{12}}\right)^2 \tag{19c}$$

Matrix failure in compression ($\sigma_2 < 0$):

$$F_m^C = \left(\frac{\sigma_2}{Y_C}\right)^2 + \left(\frac{\tau_{12}}{S_{12}}\right)^2 \tag{19d}$$

In the present study, when a failure occurs in a location, the material properties of the entire ply are reduced.

As known, when damage occurs in a composite structure, the effective material properties are reduced. This reduction can be modeled in this study by the following matrix.

$$\boldsymbol{Q}_p = \begin{bmatrix} (1-d_1)R_{11} & (1-d_1)(1-d_2)R_{12} & 0 \\ sym & (1-d_2)R_{22} & 0 \\ sym & sym & (1-d_6)R_{66} \end{bmatrix} \tag{20}$$

The parameters d_1 and d_2 are the damage factors in fiber and matrix directions, respectively and d_6 is in-plane shear component.

The material properties in Eq. (20) are defined as $R_{11}=E_1/\Delta$, $R_{22}=E_2/\Delta$, $R_{12}=(v_{12}E_1)/\Delta$, $R_{66}=G_{12}$ and $\Delta=1-v_{12}v_{21}(1-d_1)(1-d_2)$. Where E_1, E_2, G_{12}, v_{12} and v_{21} are undamaged material properties.

In the current progressive damage model, the failure of damaged material is considered to happen instantaneously. When a failure is detected in specific ply, its properties are reduced to %1 of their respective initial undamaged values.

6- Results and Discussion

The above-proposed formulations should be verified through a number of comparisons and this is done by comparing the results with those obtained by Yang [24]. To this end, the plates which are considered in this study are square plates ($a=b=500$ mm) with two types of boundary conditions as described before. Also, a uniform compressive load, N_x, is applied in the x-direction $x=a/2$ as mentioned earlier. Initial imperfection is considered to be a single half sin wave in both directions by maximum values of 0.1%, 1%, 2% and 3% of the length a in center of the plates.

Table 3. Material properties of fiber and matrix (in MPa)

Component	Value
E_1	49627
E_2	15430
v_{12}	0.272
G_{12}	4800
G_{13}	4800
G_{23}	4800
X_t	968
X_c	915
Y_t	24
Y_c	118
S_{12}	65

The composite plates under consideration are modeled as $[0/+45/+90/-45]_{X,S}$ lay-up using 8X distinct layers whose mechanical properties are listed in Table 3 as taken from Yang [24]. The parameter X takes the values of 2, 3 and 4 in this study. The thickness of each ply is considered to be equal to 1 mm and therefore, the composite laminated plates have total thickness of 16, 24 and 32 mm.

To do the convergence analysis, a composite plate with a total thickness of 16 mm is selected and analysis obtained by Hashin failure criteria. The boundary conditions are imposed as described for Type A and the plates have the maximum initial imperfection of 3%. Table 4 shows the convergence study of the ultimate strength of the plate with the number of terms N_t used in the displacement fields.

As can be seen, for the plate under consideration the convergence studies with regard to the number of terms have revealed that eight terms are sufficient to obtain the converged results. However, the number of nine terms is used to ensure an accurate convergence in all analyses. Thus, the total number of unknown coefficients is 407. Also, similar analyses were conducted with regard to the number of

Table 4. Convergence study (in MPa)

N_t	Ultimate Load
3	47.80
4	44.75
5	44.09
6	43.78
7	43.24
8	42.83
9	42.46
10	42.18

nodes for all three geometric degradation models and it was concluded that the total number of 169 nodes ($m \times n = 13 \times 13$) are sufficient to obtain the converged results.

Table 5. Results for progressive damage of composite plates for boundary condition Type A

Imp. % of a	h(mm)	σ_{LPF}(MPa)			
		Maximum stress	Tsai-Hill	Hashin	Ref [24]
0.1	16	80.34	80.25	80.34	80.69
0.1	24	167.57	166.12	167.57	168.90
0.1	32	264.88	220.38	235.64	239.28
1.0	16	56.96	56.60	56.56	57.70
1.0	24	117.69	113.61	114.02	116.50
1.0	32	184.03	172.95	174.14	177.81
2.0	16	47.71	46.55	46.24	49.47
2.0	24	99.54	99.46	99.49	100.50
2.0	32	155.22	147.43	148.84	152.59
3.0	16	43.65	42.47	42.46	45.98
3.0	24	88.67	88.46	88.53	90.42
3.0	32	136.10	131.84	131.16	133.30

Table 6. Results for progressive damage of composite plates for boundary condition Type B

Imp. % of a	h(mm)	σ_{LPF}(MPa)			
		Maximum stress	Tsai-Hill	Hashin	Hashin (Table 5)
0.1	16	100.85	100.52	100.73	80.34
0.1	24	192.75	191.61	192.37	167.57
0.1	32	329.01	223.31	277.39	235.64
1.0	16	68.17	68.11	68.11	56.56
1.0	24	142.56	141.61	141.57	114.02
1.0	32	219.72	212.12	211.73	174.14
2.0	16	60.02	59.94	59.96	46.24
2.0	24	117.33	117.61	117.32	99.49
2.0	32	177.93	174.7	174.48	148.84
3.0	16	53.48	53.58	53.42	42.46
3.0	24	100.12	99.08	98.93	88.53
3.0	32	151.02	148.60	148.32	131.16

The results for composite plates with geometrical and mechanical properties mentioned in Table 3 and two types of boundary condition (Type A and Type B) are given for different maximum initial imperfections and total thicknesses by three failure criteria.

Last Ply Failure (LPF) stresses for different composite plates with boundary condition Type A and for all three failure criteria are given in Table 5. They are compared to the results reported by Yang et al.[24]. For boundary condition Type B, LPF stresses of different composite plates for all three failure criteria are also given in Table 6.

The load-center out-of-plane displacement history (N_x-w_{tc}) and load-end shortening response (N_x-u_c) are graphically represented for composite plates having a total thickness of 32 mm and for boundary conditions Type A in Figs. 5 and 6 . The parameter w_{tc} is defined as the value of total out-of-plane displacement in the center of the plate (i.e. $w(0,0) + \bar{w}(0,0)$). Also, First Ply Failure (FPF) and LPF stresses are specified in the following figures.
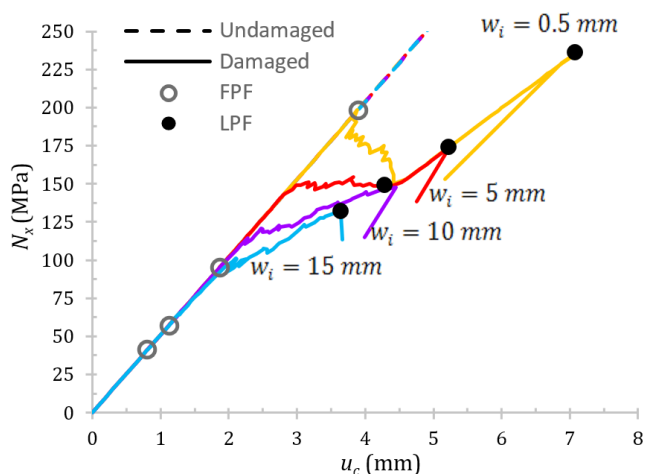

Fig. 5. Response of Load versus end shortening for 32 mm composite (Type A)
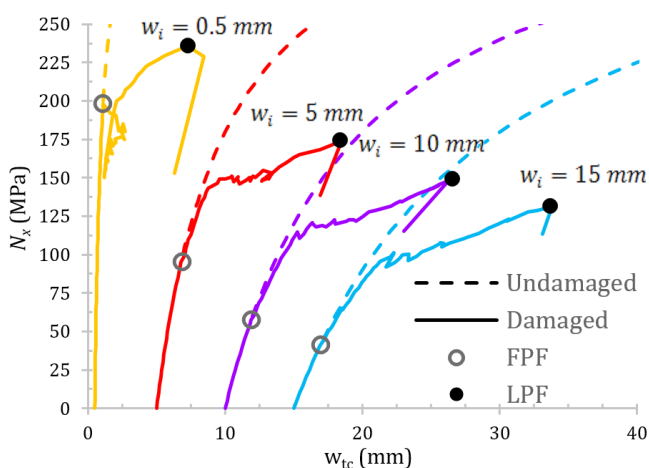

Fig. 6. Response of Load versus maximum out-of-plane displacement for 32 mm composite plates (Type A)

Table 7 shows the progressive damage behavior for the plate with a thickness of 24 mm, with the maximum initial imperfection of 1% and with boundary conditions Type A. These results have been obtained by Hashin failure criteria.

As can be seen from both tables and figures, by increasing the maximum value of initial imperfection of the plates, both FPF and LPF loads have decreased.

The response of load against center out-of-plane displacement and load against end shortening for a plate having a total thickness of 24 mm and 1% initial imperfection are plotted in Fig. 7 and Fig. 8. In these figures, the results of two types of boundary conditions are represented.
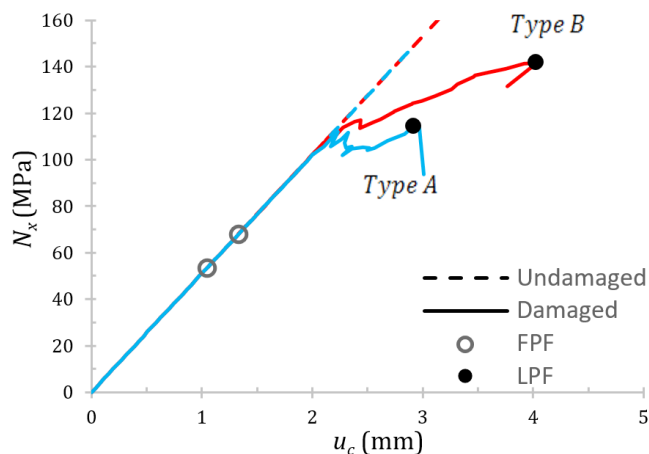

Fig. 7. Response of Load versus end shortening for 24 mm composite plates with 1% initial imperfection (Type A and Type B)
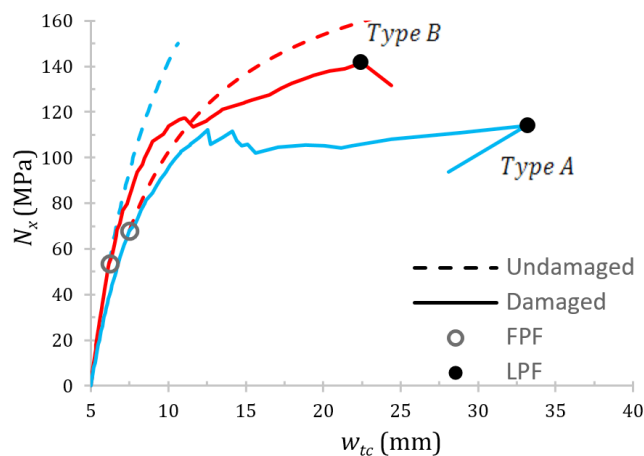

Fig. 8. Response of Load versus maximum out-of-plane displacement for 24 mm composite plates with 1% initial imperfection (Type A and Type B)

It is seen that the results obtained for the plates with boundary condition Type B have 10-20% upper ultimate loads with respect to the results obtained for Type A. This is due to the fact that the boundary conditions have significant effects on the response of imperfect composite plates and the last ply failure loads of plates having one clamped edge are greater than the corresponding values in plates with all simply-supported edges.

Also, the behavior of applied load against center out-of-plane displacement and end shortening are plotted for a plate with h=32 and 1% initial imperfection in Figs. 9 and 10. In these figures, the results obtained by Maximum stress, Tsai-Hill and Hashin failure criteria are presented.

Table 7. Progressive damage behavior for the plate with thickness of 24 mm and with %1 initial imperfection (Type A)

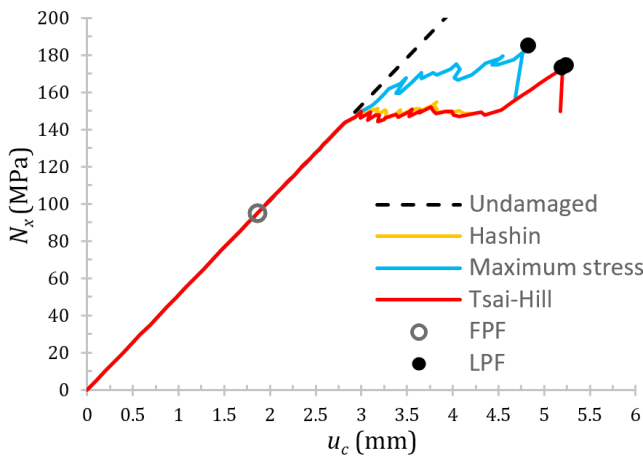| Number of failures	Number of failed ply (angle)	Coordinate of failure	Failure stress	Mode of failure
1	24(0.00)	(0,0)	**67.812 (FPF)**	Matrix Tension
2	20(0.00)	(0,0)	81.421	Matrix Tension
3	23(45.00)	(0,0)	102.579	Matrix Tension
4	16(0.00)	(0,0)	105.685	Matrix Tension
5	3(90.00)	(0,0)	112.11	Matrix Compression
6	21(-45.00)	(0,0)	105.669	Matrix Tension
7	2(45.00)	(0,0)	111.669	Matrix Compression
8	4(-45.00)	(250,250)	107.294	Matrix Tension
9	19(45.00)	(0,0)	105.064	Matrix Tension
10	1(0.00)	(250,250)	105.709	Matrix Tension
11	22(90.00)	(250,250)	101.892	Matrix Compression
12	7(90.00)	(0,0)	104.581	Matrix Compression
13	6(45.00)	(0,0)	105.418	Matrix Compression
14	5(0.00)	(-250,-250)	105.103	Matrix Tension
15	17(-45.00)	(0,0)	104.163	Matrix Tension
16	18(90.00)	(-250,-250)	105.022	Matrix Compression
17	8(-45.00)	(0,0)	108.022	Matrix Compression
18	15(45.00)	(0,0)	**114.022(LPF)**	Matrix Tension
19	1(0.00)	(0,0)	113.83	Fiber Compression
20	23(45.00)	(250,250)	93.802	Fiber Compression
21	10(45.00)	(0,0)	87.389	Matrix Compression

Fig. 9. Response of load versus end shortening, compression between failure criteria for 32 mm composite plate with %1 initial imperfection (Type A)
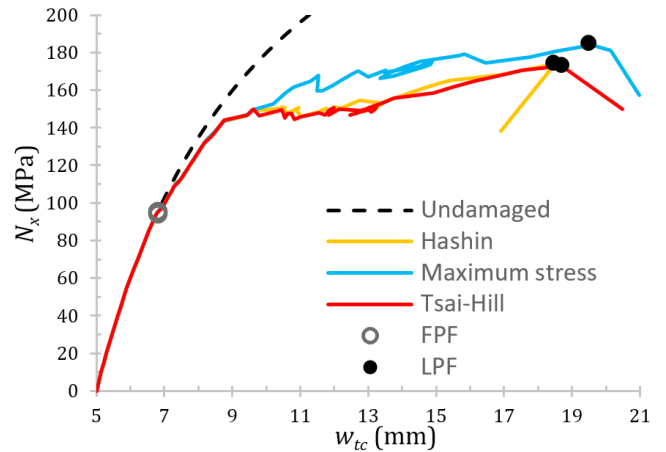

Fig. 10. Response of load versus maximum out-of-plane displacement, compression between failure criteria for 32 mm composite plate with %1 initial imperfection (Type A)

As can be seen in Table 5, the results of three failure criteria show a valid comparison with those obtained by Yang [24].

7- Conclusions

In the present paper, a new method has been developed to analyze a progressive damage of composite plate with initial imperfection under in-plane compressive load based on the discretization of the plate's domain with Legendre-Gauss-Lobatto nodes. Two types of boundary conditions were assumed for the plates. Different failure criteria have been established for the progressive damage model and results

were compared with the previous studies.

References

[1] S. Dong, K. Pister, R. Taylor, On the theory of laminated anisotropic shells and plates, *Journal of the Aerospace Sciences*, 29(8) (1962) 969-975.

[2] P.C. Yang, C.H. Norris, Y. Stavsky, Elastic wave propagation in heterogeneous plates, *International Journal of solids and structures*, 2(4) (1966) 665-684.

[3] Whitney, The effect of transverse shear deformation on

the bending of laminated plates, *Journal of Composite Materials*, 3(3) (1969) 534-547.

[4] J. Whitney, N. Pagano, Shear deformation in heterogeneous anisotropic plates, *Journal of applied mechanics*, 37(4) (1970) 1031-1036.

[5] G.J. Turvey, I.H. Marshall, *Buckling and postbuckling of composite plates*, Springer Science & Business Media, 2012.

[6] J. Argyris, L. Tenek, Recent advances in computational thermostructural analysis of composite plates and shells with strong nonlinearities, *Applied Mechanics Reviews*, 50 (1997) 285-306.

[7] Finite strip method in structural analysis. Pergamon press, (1976) 26

[8] T.G. Smith, S. Sridharan, A finite strip method for the buckling of plate structures under arbitrary loading, *International Journal of Mechanical Sciences*, 20(10) (1978) 685-693.

[9] H. Ovesy, S. Ghannadpour, G. Morada, Geometric non-linear analysis of composite laminated plates with initial imperfection under end shortening, using two versions of finite strip method, *Composite structures*, 71(3) (2005) 307-314.

[10] H. Ovesy, J. Loughlan, S. GhannadPour, Geometric non-linear analysis of channel sections under end shortening, using different versions of the finite strip method, *Computers & structures*, 84(13) (2006) 855-872.

[11] H. Ovesy, E. Zia-Dehkordi, S. Ghannadpour, High accuracy post-buckling analysis of moderately thick composite plates using an exact finite strip, *Computers & Structures*, 174 (2016) 104-112.

[12] R, Liu. Meshfree methods: *moving beyond the finite element method*. Taylor & Francis, (2009)

[13] K. Liew, Y. Huang, Bending and buckling of thick symmetric rectangular laminates using the moving least-squares differential quadrature method, *International Journal of Mechanical Sciences*, 45(1) (2003) 95-114.

[14] K. Liew, J. Wang, M. Tan, S. Rajendran, Postbuckling analysis of laminated composite plates using the mesh-free kp-Ritz method, *Computer methods in applied mechanics and engineering*, 195(7) (2006) 551-570

[15] K.M. Liew, X. Zhao, A.J. Ferreira, A review of meshless methods for laminated and functionally graded plates and shells, *Composite Structures*, 93(8) (2011) 2031-2041.

[16] S. Ghannadpour, M. Barekati, Initial imperfection effects on postbuckling response of laminated plates

under end-shortening strain using Chebyshev techniques, *Thin-Walled Structures*, 106 (2016) 484-494.

[17] N. Jaunky, D.R. Ambur, C.G. Dávila, M. Hilburger, D.M. Bushnell, *Progressive failure studies of composite panels with and without cutouts*, (2001).

[18] L. Brubak, J. Hellesland, E. Steen, Semi-analytical buckling strength analysis of plates with arbitrary stiffener arrangements, *Journal of Constructional Steel Research*, 63(4) (2007) 532-543.

[19] L. Brubak, J. Hellesland, Approximate buckling strength analysis of arbitrarily stiffened, stepped plates, *Engineering Structures*, 29(9) (2007) 2321-2333.

[20] L. Brubak, J. Hellesland, Semi-analytical postbuckling and strength analysis of arbitrarily stiffened plates in local and global bending, *Thin-Walled Structures*, 45(6) (2007) 620-633.

[21] L. Brubak, J. Hellesland, Strength criteria in semi-analytical, large deflection analysis of stiffened plates in local and global bending, *Thin-Walled Structures*, 46(12) (2008) 1382-1390.

[22] A. Orifici, R. Thomson, R. Degenhardt, A. Kling, K. Rohwer, J. Bayandor, Degradation investigation in a postbuckling composite stiffened fuselage panel, *Composite Structures*, 82(2) (2008) 217-224.

[23] B. Hayman, C. Berggreen, C. Lundsgaard-Larsen, A. Delarche, H. Toftegaard, R. Dow, J. Downes, K. Misirlis, N. Tsouvalis, C. Douka, Studies of the buckling of composite plates in compression, *Ships and Offshore Structures*, 6(1-2) (2011) 81-92.

[24] Q.J. Yang, B. Hayman, H. Osnes, Simplified buckling and ultimate strength analysis of composite plates in compression, *Composites Part B: Engineering*, 54 (2013) 343-352.

[25] Q.J. Yang, B. Hayman, Prediction of post-buckling and ultimate compressive strength of composite plates by semi-analytical methods, *Engineering Structures*, 84 (2015) 42-53.

[26] Q.J. Yang, B. Hayman, Simplified ultimate strength analysis of compressed composite plates with linear material degradation, *Composites Part B: Engineering*, 69 (2015) 13-21.

[27] J.N. Reddy, *Mechanics of laminated composite plates and shells: theory and analysis*. CRC press. (2004)

[28] E.J. Barbero, *Introduction to Composite Materials Design*. Taylor & Francis. (1998)